Published in final edited form as:
Science. 2008 December 5; 322(5907): 1543–1546. doi:10.1126/science.1163086.

Inhibition of Rac by the GAP activity of Centralspindlin is Essential for Cytokinesis

Julie C. Canman[1,*,3], **Lindsay Lewellyn**[1], **Kimberley Laband**[1], **Stephen J. Smerdon**[2], **Arshad Desai**[1], **Bruce Bowerman**[3,◆], and **Karen Oegema**[1,◆]

[1] Ludwig Institute for Cancer Research, UCSD, La Jolla, CA, 92093

[2] National Institute for Medical Research, The Ridgeway, Mill Hill, London NW7 1AA, UK

[3] Institute for Molecular Biology, University of Oregon, Eugene, OR, 97403

Abstract

During cytokinesis, the small GTPase RhoA orchestrates contractile ring assembly and constriction. RhoA signaling is controlled by the central spindle—a set of microtubule bundles that forms between the separating chromosomes. Centralspindlin, a protein complex consisting of the kinesin-6 ZEN-4, and the Rho GAP CYK-4, is required for central spindle assembly and cytokinesis. However, the importance of the CYK-4 GAP activity and whether it regulates RhoA remains unclear. Here, we show that two separation-of-function mutations in the GAP domain of *C. elegans* CYK-4 lead to cytokinesis defects that mimic Centralspindlin loss-of-function. These defects can be rescued by depletion of Rac or its effectors, but not RhoA. Our findings suggest that inactivation of Rac by Centralspindlin functions in parallel with RhoA activation to drive cytokinesis.

Cytokinesis completes mitosis, partitioning a single cell into two. To coordinate cell division with chromosome segregation, the anaphase spindle directs the assembly and constriction of a contractile ring composed of filamentous-actin and myosin II that physically divides the cell (1). Understanding how the anaphase spindle communicates with the cell cortex during cytokinesis is a major current challenge. Anaphase spindle signaling is mediated by activation of the small GTPase RhoA (1,2). Consistent with a central role in cytokinesis, RhoA and its activating GEF, ECT-2, are essential for contractile ring assembly and constriction (3–5).

RhoA signaling is controlled by the central spindle- an array of anti-parallel microtubule bundles that forms between the separating chromosomes during anaphase (1). Centralspindlin, a conserved heterotetrameric complex consisting of two molecules of kinesin-6 (ZEN-4 in *C. elegans*) and two molecules of a protein containing a GAP domain that targets Rho family GTPases (CYK-4 in *C. elegans*), is critical for central spindle assembly and contractile ring constriction (1,6). The current dominant model proposes that Centralspindlin contributes directly to the equatorial activation of RhoA by targeting ECT-2 to the central spindle (3,4, 7). Formation of the hetero-tetrameric Centralspindlin complex requires an interaction between the central region of ZEN-4 and the N-terminal region of CYK-4 (Fig. 1A) (6,8). Mutant forms of CYK-4 and ZEN-4 that disrupt Centralspindlin assembly lead to a cytokinesis phenotype similar to that resulting from depletion of Centralspindlin subunits by RNAi (Fig. 1)—failure to form a central spindle accompanied by a defect in contractile ring constriction (9–12).

Correspondence and requests for materials should be addressed to: jcanman@ucsd.edu or koegema@ucsd.edu, Phone: (858) 534-9576, Fax: (858) 534-7750.
◆Authors contributed equally to this work
*Current address

The CYK-4 C-terminus contains a conserved GAP domain, predicted to inactivate Rho family GTPases (Fig. 1A) (11). The role of this domain in cytokinesis and the identity of the Rho family GTPase that it targets are unknown (11,13–15). *In vitro*, the GAP domains of CYK-4 and its homologs are active towards all three subclasses of Rho family GTPases: RhoA, Rac, and CDC-42 (11,16,17). However, since RhoA is the only family member essential for cytokinesis, it is assumed that Centralspindlin GAP activity acts on RhoA by either promoting RhoA cycling (18), or by inactivating RhoA after cytokinesis to promote contractile ring disassembly (1). However, it is also possible that RhoA is not the critical target of the CYK-4 GAP domain. Supporting this hypothesis, haplo-insufficiency of Rac can suppress the rough-eye phenotype induced by RNAi of the *Drosophila* CYK-4 homolog (although cytokinesis was not examined) (14), suggesting that in some contexts CYK-4 may oppose Rac activation.

To study the role of the GAP domain in cytokinesis (19), we characterized two *C. elegans* mutants containing amino acid substitutions within the CYK-4 GAP domain (Fig. 1A,B). Both were independently isolated using a forward genetics approach to identify conditional, embryonic-lethal alleles (20). The two mutations result in a Glu to Lys change at residue 448 (CYK-4$^{GAP(E448K)}$) and a Thr to Ile change at residue 546 (CYK-4$^{GAP(T546I)}$) respectively (Fig. 1A). Based on the X-ray structure of the human CYK-4 homolog (PDBID: 2OVJ), the Glu to Lys substitution would lead to a charge reversal, disrupting the network of salt-bridge and hydrogen-bond interactions that positions the arginine-finger (Arg 459), a conserved structural motif essential for GAP activity (Fig. 1B) (17,21,22). Although the effects of the Thr to Ile substitution are less clear, the additional methyl group on the isoleucine likely results in steric clashes with surrounding residues, causing a conformational change that also interferes with arginine-finger positioning. Both alleles are strictly recessive (Fig. S1), temperature-sensitive, and fast-inactivating. Within one minute of shifting to the restrictive temperature (25°C), a fully penetrant failure of the first embryonic cytokinesis was observed in both mutants. Thus, we conclude that these are loss-of-function alleles affecting the CYK-4 GAP domain.

We used quantitative live imaging assays to characterize cytokinesis in mutant embryos at the restrictive-temperature. We found no difference in the levels or distribution of cortical myosin II, assayed by monitoring a GFP fusion with the myosin II heavy chain NMY-2, during the initial stages of contractile ring assembly in any of the GAP or Centralspindlin-assembly (CSA) mutants (Fig. S2B,C). However, after the contractile ring constricted to form a furrow, the GAP domain mutants exhibited a severe ingression defect. The rate of furrow ingression, measured in embryos expressing a GFP-labeled plasma membrane marker, was ~3 fold slower than that in control embryos, and furrows only ingressed to ~50% of the initial cell diameter before regressing. Importantly, this ingression defect mimicked that in the Centralspindlin-assembly mutants and in embryos depleted of CYK-4 by RNAi (12) (Fig. 1C,D; S3C; Movie S1). In all Centralspindlin mutants, levels of myosin II at the leading edge of the furrow were reduced to ~60% of those in controls (Fig. S3A,B). However, it is unclear whether this is a cause or a consequence of the reduced ingression rate. Together, these results suggest that the CYK-4 GAP domain is fundamental to the role of Centralspindlin in promoting furrow ingression.

Centralspindlin is also required for assembly of the central spindle (9–11). Therefore, we next examined central spindle structure in the GAP mutant embryos. In contrast to the lack of a central spindle in *zen-4(RNAi)* embryos, immunofluorescence analysis of GAP mutant embryos revealed no apparent defects in central spindle organization or ZEN-4 targeting (Fig. 2A). Time-lapse imaging of embryos expressing a GFP fusion with AuroraB^{AIR-2} kinase (the enzymatic component of the Chromosomal Passenger Complex) confirmed that central spindle structure was not affected in the GAP mutants (Fig. 2B;Movie S2). In *C. elegans* embryos, the centrosomes separate abruptly following anaphase onset when central spindle structure is

disrupted (23). However, the kinetics of centrosome separation in the GAP mutants were identical to those in controls, confirming that the mechanical integrity of the central spindle was intact (Fig. 2C). Thus, CYK-4$^{GAP(E448K)}$ and CYK-4$^{GAP(T546I)}$ are separation-of-function mutants that uncouple the role of CYK-4 in furrow ingression from its role in central spindle assembly. As the cytokinesis defects observed in the GAP mutants are similar to those resulting from disrupting Centralspindlin assembly or depletion of its components, we conclude that the GAP domain of Centralspindlin is essential for furrow ingression.

As CYK-4 GAP activity is expected to down-regulate a Rho family GTPase, we reasoned that RNAi-mediated depletion of the target GTPase would rescue the cytokinesis defect in CYK-4$^{GAP(E448K)}$ embryos. There are five Rho family members in *C. elegans*: RhoA^{RHO-1}, Rac^{CED-10}, Rac^{RAC-2}, RhoG^{MIG-2}, and CDC-42 (24). Because depletion of RhoA^{RHO-1} results in a cytokinesis defect on its own, we tested if partial depletion of RhoA^{RHO-1} or its activating GEF (ECT-2) could suppress the mutant phenotype. Instead, partial depletion of either RhoA^{RHO-1} or ECT-2 enhanced the CYK-4$^{GAP(E448K)}$ cytokinesis phenotype suggesting that RhoA^{RHO-1} is not the main target of CYK-4 GAP activity (Fig. 3A,B;Fig. S4A). We next investigated whether depletion of other Rho family members could rescue the CYK-4$^{GAP(E448K)}$ phenotype. Individual depletions of Rac^{CED-10}, Rac^{RAC-2}, RhoG^{MIG-2}, and CDC-42 did not have any detectable effect on cytokinesis (Fig. 3C). Depletion of CDC-42 or RhoG^{MIG-2} also did not ameliorate the cytokinesis phenotype in CYK-4$^{GAP(E448K)}$ embryos (Fig 3A,C,D). In contrast, depletion of the Rac homologs significantly rescued the CYK-4$^{GAP(E448K)}$ cytokinesis phenotype. RNAi depletion of Rac^{CED-10} and Rac^{RAC-2} allowed 70% and 24%, respectively, of CYK-4$^{GAP(E448K)}$ embryos to successfully complete the first cytokinesis (Fig. 3A,C,D). Due to two (30–40 bp) stretches of identity at the nucleotide level we cannot rule out that RNAi depletion of Rac^{CED-10} also targets Rac^{RAC-2} (albeit less-efficiently) and vice versa. Double depletion of Rac^{CED-10} and Rac^{RAC-2} by RNAi did not increase the efficiency of rescue over that observed following depletion of Rac^{CED-10} alone (Fig. S4D). Cumulatively, these results suggest that CYK-4 GAP activity promotes furrow ingression by down-regulating Rac. In agreement with a role for CYK-4 in the equatorial down-regulation of Rac, a FRET probe in mammalian cells revealed a localized reduction in active Rac at the cell equator during cytokinesis that was eliminated by over-expressing a GAP dead mutant of the CYK-4 homolog (25).

If the GAP activity of CYK-4 is critical for the role of Centralspindlin in furrow ingression, we would expect Rac^{CED-10} depletion to also rescue the lack of furrow ingression resulting from inhibiting Centralspindlin assembly. Consistent with this hypothesis, 85% of furrows in ZEN-4$^{CSA(D520N)}$ embryos ingressed fully when Rac^{CED-10} was depleted (Fig. S4B). However, Rac^{CED-10} depletion was less efficient in rescuing cytokinesis completion with the ZEN-4$^{CSA(D520N)}$ mutant compared to the GAP mutant (Fig. S4B). This result suggests an additional role for either Centralspindlin or the central spindle in the completion of cytokinesis that is independent of the GAP activity. Importantly, Rac^{CED-10} depletion had no effect on furrow ingression in AuroraB$^{AIR-2(P265L)}$ embryos which have a similar spectrum of defects in central spindle assembly and furrow ingression to that resulting from Centralspindlin disruption (12) (Fig. S4C), confirming the specificity of the rescue. Cumulatively, our results indicate that negative regulation of Rac activity by Centralspindlin is essential for its role in promoting furrow ingression.

Why is inhibition of Rac signaling important for contractile ring constriction? Rac has been shown to promote activation of the Arp2/3 complex via activators WASP^{WSP-1} and WAVE^{WVE-1}, resulting in the formation of a branched meshwork of short cross-linked actin filaments (26). One possibility is that these Rac effectors interfere with actin filaments nucleated by the cytokinesis formin, CYK-1, which function with myosin II to drive cytokinesis. To test this idea, we determined whether depletion of WASP^{WSP-1}/

WAVE^{WVE-1} or the Arp2/3 complex could also rescue cytokinesis in CYK-4$^{GAP(E448K)}$ embryos (27,28) (Fig. 4A,B). Although their individual depletions did not dramatically suppress the cytokinesis defect in CYK-4$^{GAP(E448K)}$ embryos, co-depletion of WASP^{WSP-1} and WAVE^{WVE-1} led to significant rescue (Fig 4A); 72% of furrows ingressed fully and 43% of embryos successfully completed cytokinesis (Fig 4A). RNAi of Arp2^{ARX-2}, also significantly suppressed the CYK-4$^{GAP(E448K)}$ cytokinesis defect, with 74% of furrows ingressing fully and 52% of embryos completing division (Fig. 4B). Thus, one important consequence the down-regulation of Rac activity by CYK-4 is to inhibit Rac-mediated activation of the Arp2/3 complex.

In summary, we have uncovered a negative regulation cascade that is essential for successful cytokinesis. Although negative regulation has been proposed to be important during cytokinesis, previous models have emphasized inhibition of cortical contractility by astral microtubules that contact the polar regions of the cell (29,30). Negative regulation of an inhibitory pathway at the cell equator has not been widely considered. Our findings lead to a new model for cytokinesis signaling in which inactivation of Rac by CYK-4 functions in parallel with RhoA activation to drive contractile ring constriction during cytokinesis (Fig. 4C). Active Arp2/3 complex in the furrow region may disrupt contractile ring constriction by branching formin-nucleated actin. Alternatively, active Arp2/3 complex could nucleate the formation of an independent branched actin network that competes for essential contractile ring components, or presents a structural barrier to furrow ingression. Further work will be needed to distinguish between these possibilities and elucidate the overlap between the positive and negative regulation of contractility that guides cortical remodeling during cell division. (31)

Materials and Methods

Mutant cloning and rescue experiments

The *cyk-4(or570ts)* and *cyk-4(or749ts)* (CYK-4$^{GAP(T546I)}$ and CYK-4$^{GAP(E448K)}$, respectively) mutants were isolated in EMS and ENU mutagenesis screens, respectively, for conditional (temperature-sensitive) embryonic-lethal mutants as described (1,2). The mutations were mapped to LG::III using strains *MT3751* and *MT464*. Mutations were identified by sequencing, after refining their location by 3-factor visible marker mapping as described (3) using strains *DR104* and *CB2053* for *cyk-4(or570ts*) and *cyk-4(or749ts)* respectively. To confirm that the *cyk-4* mutations were the cause of the cytokinesis defect, we rescued the embryonic lethality by expression of a GFP fusion with CYK-4. To test for rescue, the *cyk-4 (or570ts)* and *cyk-4(or749ts)* mutants were crossed with *WH0279* non-Unc hermaphrodites. First, *cyk-4(or749ts)* and *cyk-4(or570ts)* were linked to *unc-119(ed3)* and homozygosed then, *ojIs12[cyk-4::GFP unc-119(+)]/+* (which is lethal when homozygous) progeny were screened for the ability to rescue embryonic lethality at restrictive temperature. Both *cyk-4(or570ts)* and *cyk-4(or749ts)* were back-crossed six times prior to mating into fluorescent protein expressing strains for phenotypic analysis (*him-8(e1489)* first cross, N2 remaining out-crosses). All analysis was done in non-Him strains to avoid possible phenotypic complications.

Temperature control

Strains were maintained at the permissive temperature of 16°C. For all live imaging experiments, the temperature was controlled by heating the room to 26°C for at least one hour prior to filming or until the microscope temperature reached 26°C. Embryos were maintained at 16°C until immediately prior to filming. The temperature was continuously monitored during filming using a thermometer probe wedged into the microscope body near the stage. For some experiments, a heated stage was also used (20/20 Technology Inc, Wilmington, NC).

Imaging and quantitative analysis

Live imaging was performed on newly fertilized embryos mounted on agarose pads as previously described (4). Embryos were filmed using a spinning disk confocal as described (5) using a 60x, 1.4 NA PlanApochromat lens with 2×2 binning. For all movies, Differential Interference Contrast (DIC) images and/or images of an $RFP^{mCherry}$ fusion with histone H2B were collected in parallel to monitor cell cycle progression. The rate of furrow ingression was measured in strains expressing a GFP labeled plasma membrane probe. A z-series consisting of 14 planes at 2.5μm intervals was collected every 20s and the data from the equatorial region of the embryo was isolated, rotated by 90°, and projected to generate an "end on" view that was used to measure furrow diameter. To test for suppression of the mutant phenotype, central plane images of mutant embryos depleted of the indicated protein by RNAi were collected at 10s intervals. GFP::$AuroraB^{AIR-2}$ was imaged by collecting 5 z-planes at 1.5 μm intervals every 10s.

NMY-2::GFP (Myosin II heavy chain) was imaged by acquiring 4 z-planes at 1 μm intervals at the cell cortex, followed by a single central plane image every 10s. Analysis of the post-anaphase accumulation of cortical NMY-2::GFP as a function of embryo length was performed on maximum-intensity projections of the cortical z-series. A line bisecting the embryo was drawn from the anterior to the posterior tip of the embryo, and MetaMorph software (Molecular Devices, Downingtown, PA) was used to generate an average intensity line scan (50 pixels wide ~1/2 of the width of the embryo) for each time point. Embryos were divided into 20 equal length segments from anterior (0% embryo length) to posterior (100% embryo length), and the mean NMY-2::GFP in each segment was calculated for each time point, after subtraction of a background measurement for that segment made just prior to anaphase onset. The values for each data set were normalized by dividing all intensity values by the average maximum value for controls (55–65% embryo width). The amount of NMY-2::GFP in the contractile ring at the leading edge of the ingressing furrow was quantified using the central plane images as outlined in Fig. S3A.

Immunofluoresence and imaging fixed embryos

Methanol fixation was performed as described (6) on worms that were pre-shifted to restrictive temperature for 1–2 hours, and dissection was done in a 26°C room. Images were acquired as described (7) using a Deltavision microscope equipped with a 100x Plan Apo 1.35 N.A. objective. All antibodies were used at a concentration of 1μg/ml.

RNAi

dsRNA was made as described (6). After injection, worms were allowed to recover for 44–48 hrs at 16°C prior to filming unless the dsRNA led to sterility in which case the worms were allowed to recover for 12–15 hrs (*ect-2*), 22–24 hrs (*cyk-4*), and 36–38 hrs (*rho-1*), respectively.

Supplementary Material

Refer to Web version on PubMed Central for supplementary material.

References and Notes

1. Glotzer M. Science Mar 18;2005 307:1735. [PubMed: 15774750]
2. Bement WM, Benink HA, von Dassow G. J Cell Biol Jul 4;2005 170:91. [PubMed: 15998801]
3. Nishimura Y, Yonemura S. J Cell Sci Jan 1;2006 119:104. [PubMed: 16352658]
4. Yuce O, Piekny A, Glotzer M. J Cell Biol Aug 15;2005 170:571. [PubMed: 16103226]
5. Kamijo K, et al. Mol Biol Cell Jan;2006 17:43. [PubMed: 16236794]
6. Mishima M, Kaitna S, Glotzer M. Dev Cell Jan;2002 2:41. [PubMed: 11782313]

7. Somers WG, Saint R. Dev Cell Jan;2003 4:29. [PubMed: 12530961]
8. Pavicic-Kaltenbrunner V, Mishima M, Glotzer M. Mol Biol Cell Dec;2007 18:4992. [PubMed: 17942600]
9. Raich WB, Moran AN, Rothman JH, Hardin J. Mol Biol Cell Aug;1998 9:2037. [PubMed: 9693365]
10. Powers J, Bossinger O, Rose D, Strome S, Saxton W. Curr Biol Oct 8;1998 8:1133. [PubMed: 9778533]
11. Jantsch-Plunger V, et al. J Cell Biol Jun 26;2000 149:1391. [PubMed: 10871280]
12. Severson AF, Hamill DR, Carter JC, Schumacher J, Bowerman B. Curr Biol Oct 5;2000 10:1162. [PubMed: 11050384]
13. Minoshima Y, et al. Dev Cell Apr;2003 4:549. [PubMed: 12689593]
14. D'Avino PP, Savoian MS, Glover DM. J Cell Biol Jul 5;2004 166:61. [PubMed: 15240570]
15. Yamada T, Hikida M, Kurosaki T. Exp Cell Res Nov 1;2006 312:3517. [PubMed: 16959247]
16. Toure A, et al. J Biol Chem Mar 13;1998 273:6019. [PubMed: 9497316]
17. Kawashima T, et al. Blood Sep 15;2000 96:2116. [PubMed: 10979956]
18. Bement WM, Miller AL, von Dassow G. Bioessays Oct;2006 28:983. [PubMed: 16998826]
19. Methods can be found in supplementary online material.
20. Encalada SE, et al. Dev Biol Dec 15;2000 228:225. [PubMed: 11112326]
21. Ahmed S, et al. J Biol Chem Jul 1;1994 269:17642. [PubMed: 8021274]
22. Rittinger K, Walker PA, Eccleston JF, Smerdon SJ, Gamblin SJ. Nature Oct 16;1997 389:758. [PubMed: 9338791]
23. Oegema K, Desai A, Rybina S, Kirkham M, Hyman AA. J Cell Biol Jun 11;2001 153:1209. [PubMed: 11402065]
24. Lundquist, EA. The C. elegans Research Community, WormBook. 2006. WormBook, edhttp://www.wormbook.org
25. Yoshizaki H, et al. J Cell Biol Jul 21;2003 162:223. [PubMed: 12860967]
26. Pollard TD. Annu Rev Biophys Biomol Struct 2007;36:451. [PubMed: 17477841]
27. Severson AF, Baillie DL, Bowerman B. Curr Biol Dec 23;2002 12:2066. [PubMed: 12498681]
28. Withee J, Galligan B, Hawkins N, Garriga G. Genetics Jul;2004 167:1165. [PubMed: 15280232]
29. Rappaport, R. Cambridge University Press; Cambridge, UK: 1997.
30. Dechant R, Glotzer M. Dev Cell Mar;2003 4:333. [PubMed: 12636915]

31. We thank all members of the Oegema, Desai, and Bowerman labs. We thank Amy Maddox, Julien Dumont, and Rebecca Green for reading this manuscript; Julien Dumont for making dsRNAs; and Yuji Kohara for cDNA clones. J.C.C. was funded by the JCC-MF and by the LLS. L.L. was supported by the NIH/NIGMS (T32 GM008666) and by the NCI. K.O. and A.D. were funded by the LICR. B.B. was funded by the NIH (GM058017).

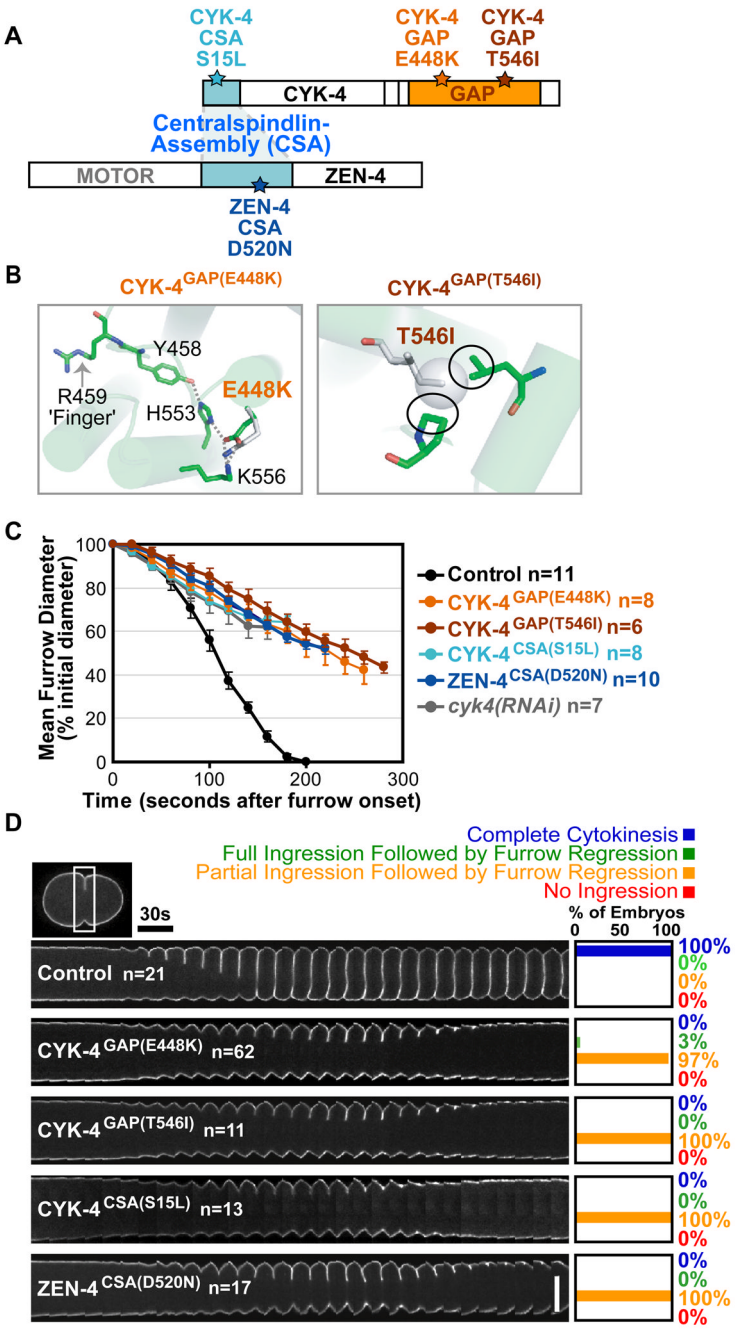

Figure 1. CYK-4 GAP domain mutants phenocopy Centralspindlin loss-of function

A) Residues changed in CYK-4 and ZEN-4 mutant proteins. **B)** The E448K and T546I substitutions destabilize CYK-4 GAP domain structure. **C)** Plot of mean furrow diameter versus time. Error bars=SEM. **D)** Time-lapse montage of the furrow region in embryos expressing a GFP::plasma membrane marker. Series begin at anaphase onset. Scale bar, 20μm.

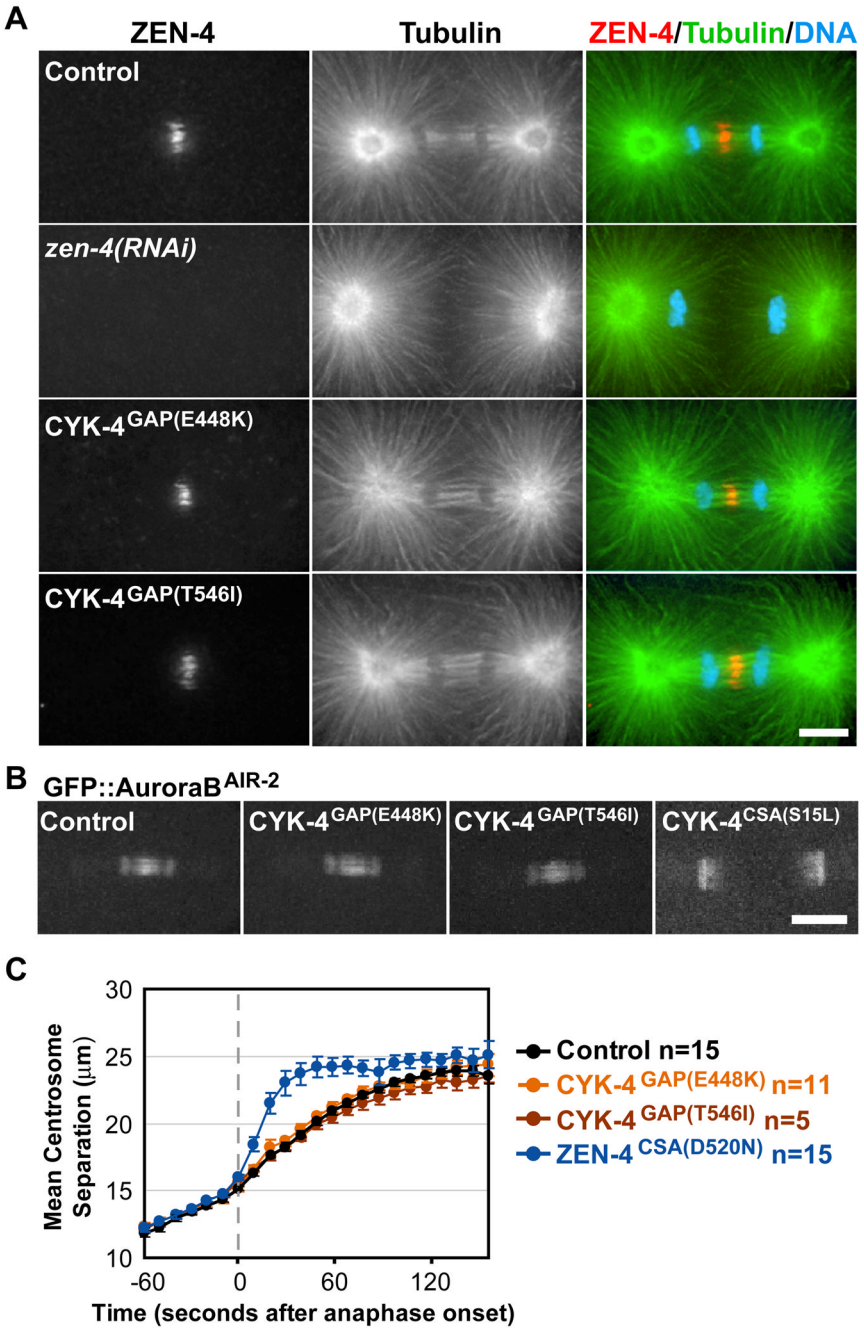

Figure 2. Central spindle assembly is not disrupted in the GAP mutants

A) Immunofluorescence staining for tubulin, ZEN-4, and DNA. **B)** Images of GFP::AuroraB^{AIR-2} 40s post-anaphase onset. **C)** Plot of mean centrosome separation verses time. Error bars=SEM. Scale bars, 10 μm.

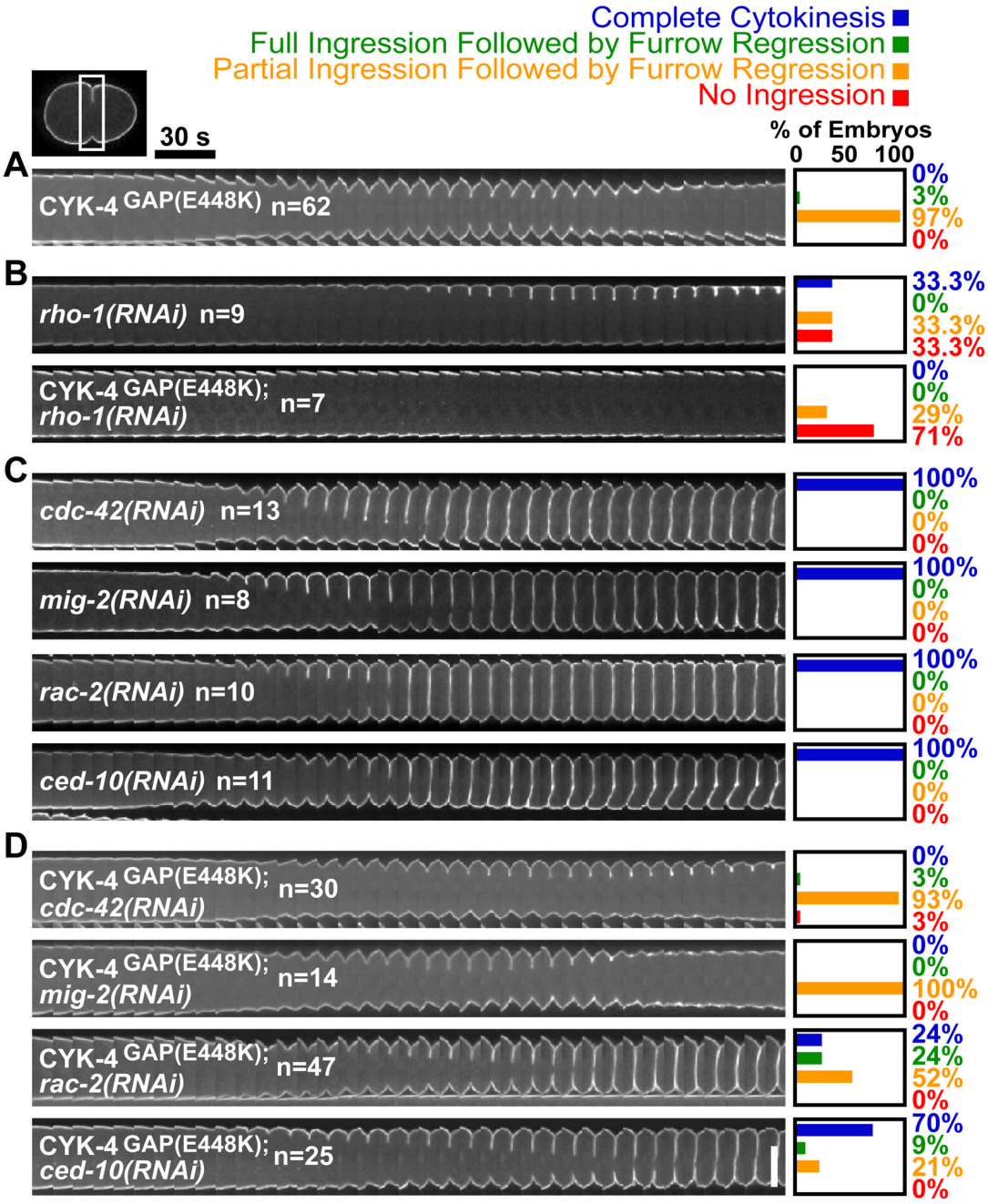

Figure 3. Rac depletion suppresses the cytokinesis defect in CYK-4$^{GAP(E448K)}$ embryos

Time-lapse montage of the furrow region in embryos expressing a GFP::plasma membrane marker. Series begin at anaphase onset. **A**) CYK-4$^{GAP(E448K)}$ embryos exhibit partial furrow ingression followed by regression. **B**) Partial depletion of RhoA^{RHO-1} enhances the CYK-4$^{GAP(E448K)}$ cytokinesis defect. **C**) RNAi of other Rho family members does not disrupt cytokinesis. **D**) Depletion of Rac^{CED-10} or Rac^{RAC-2} rescues cytokinesis success in CYK-4$^{GAP(E448K)}$ embryos. Scale bar, 20 μm.

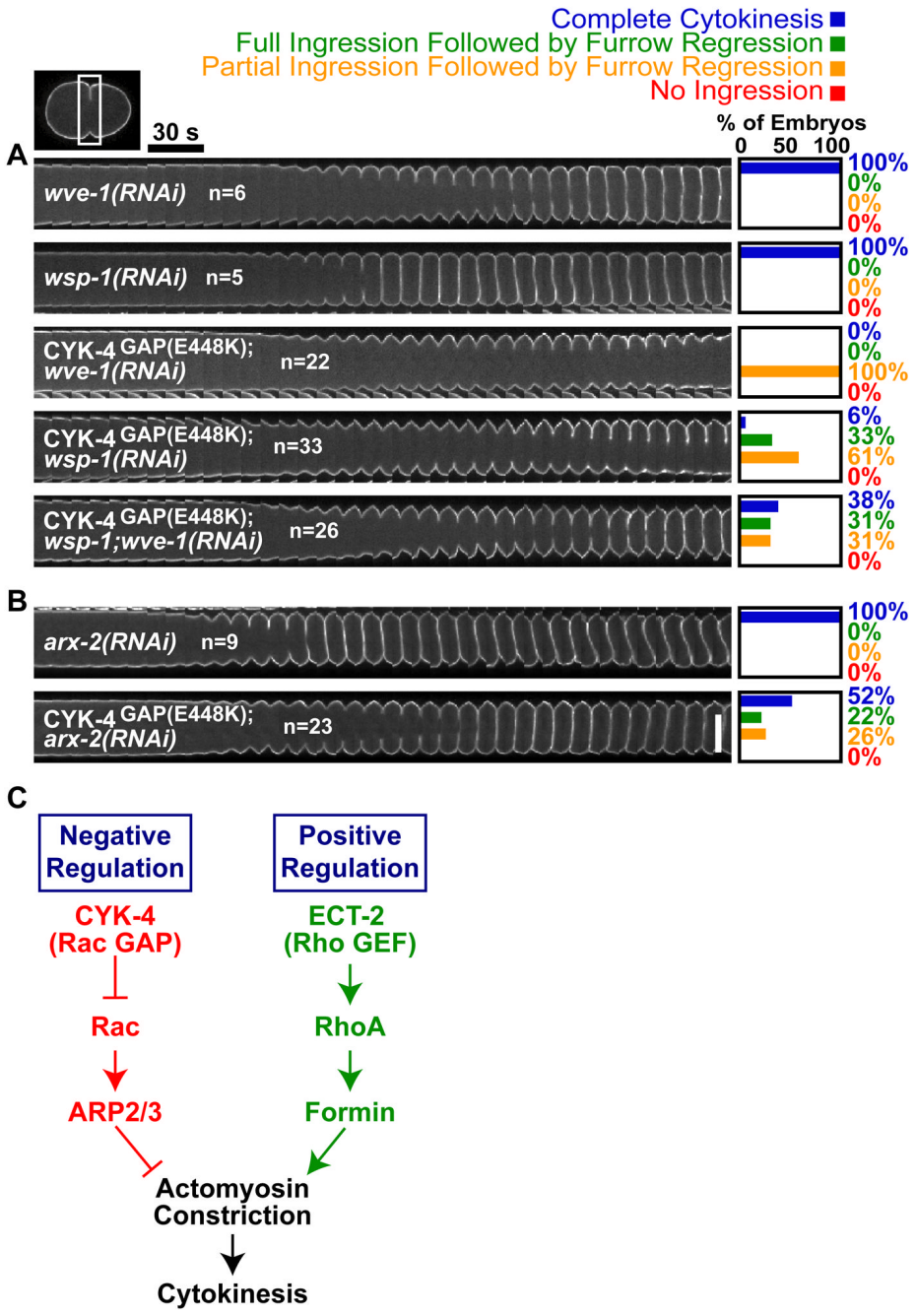

Figure 4. Negative regulation of Rac, WASP/WAVE, and the Arp2/3 complex by CYK-4 is essential for cytokinesis

Cytokinesis in CYK-4$^{GAP(E448K)}$ embryos is rescued by co-depletion of **A)** the Rac effectors WASP^{WSP-1}/WAVE^{WVE-1} or **B**) of the downstream target Arp2^{ARX-2}. Scale bar, 20 μm. **C)** Model for signaling during cytokinesis.